Train-to-Train Short Range Communication and Relative Localization based on IEEE802.15.4

Paul Unterhuber, Martin Schmidhammer, Christian Gentner, Benedikt Merk, Benjamin Siebler,
Andreas Lehner, Fabian de Ponte Müller, Ibrahim Rashdan, Dominik Egginger
Institute of Communications and Navigation, German Aerospace Center (DLR), Oberpfaffenhofen,
82234 Wessling, Germany, paul.unterhuber@dlr.de

***Abstract*—The advancement of autonomous rail operations, particularly in the context of virtually coupled train set (VCTS) and self driving freight wagon (SDFW), demands reliable, real-time, and infrastructure-independent communication and localization between rail vehicles. Current solutions often rely on fixed infrastructure or technologies with limited accuracy and resilience. This poses a critical challenge in achieving the high levels of safety, availability, and precision required for decentralized train coordination. This work addresses the challenge by evaluating a train-to-train (T2T) communication system based on IEEE 802.15.4 in real-world railway settings. A comparative assessment of omni-directional and directional antenna configurations was conducted to evaluate their impact on system performance. The results demonstrate that T2T short-range communication (SRC) and relative localization (RL) enables reliable high throughput data exchange and accurate radio-based ranging in the test range between 0 and 250 m. Directional antennas significantly enhance signal stability by mitigating interference, while omni-directional configurations maintained sufficient performance for operational use. The system proved resilience to environmental challenges, supporting safe and scalable coordination of rail vehicles in dynamic scenarios. These achievements validate the feasibility of a decentralized communication and localization framework, paving the way for autonomous trains, VCTSs and SDFWs.**

***Index Terms*—train-to-train, short-range communication, relative localization, IEEE 802.15.4, railway tests, VCTS**

I. Introduction

The global transportation sector is undergoing a profound transformation driven by digitalization, the pursuit of higher automation levels, and the urgent need to reduce carbon dioxide emissions. Within this context, the railway industry is actively exploring innovative operational solutions to enhance efficiency, capacity, and sustainability. Among these, automatic train operation (ATO), remote train operation (RTO), SDFWs, and VCTSs represent paradigm-shifting solutions that promise to redefine how trains are operated and coordinated [1]. A critical enabler of these advanced operational models is reliable wireless communication within trains, between train units or even across different trains. In particular, VCTSs rely on wireless communications to maintain coordinated movement among multiple train units without physical coupling. This requires a communication system capable of delivering low latency, high reliability, and high data integrity to ensure safe and stable platoon control. To meet these stringent demands, a multi-layered communication architecture is emerging, combining T2T communication with train-to-ground links, such as the future railway mobile communication system (FRMCS) to support centralized coordination and traffic management.

T2T communication can be realized through various wireless standards, each offering distinct trade-offs in terms of data rate, latency, frequency allocation, and communication range. The selection of an appropriate communication standard depends on the specific operational requirements. While cellular based systems like 3GPP LTE or 5G-NR provide large coverage, they may not meet the low latency and high reliability demands for real-time control within a VCTS. In contrast, T2T SRC technologies, particularly those based on high-bandwidth and low-latency protocols have gained increasing attention for their suitability for safety critical applications.

Recent years have seen extensive testing of various communication standards in railway contexts, including ETSI TETRA [2], IEEE 802.11p (ITS-G5) [3], and 3GPP LTE-V2X [4]. However, with the growing interest in joint communication and sensing capabilities, newer standards offering large bandwidth such as IEEE 802.15.4 (below 10 GHz), 3GPP 5G-NR, and IEEE 802.11bd, are attracting significant interest. These technologies enable high-resolution radio-based ranging, a key component for maintaining safe inter-vehicle distances. Despite their advantages, high-frequency systems face practical limitations in communication range due to stringent transmit power regulations and high path loss at high frequencies.

Among the available standards, IEEE 802.15.4 stands out due to its support of bandwidths of 500 MHz or 1 GHz, built-in radio ranging capabilities, and availability of commercial off-the-shelf (COTS) components. Originally designed for indoor applications, its performance in outdoor, dynamic railway environments remained unexplored so far. Therefore, a dedicated test campaign was conducted to evaluate the feasibility and performance of IEEE 802.15.4 based SRC and RL in a real-world railway setting. First details about the preparation of the test system and the tests were presented in [5]. This paper presents the design of the test architecture, the execution of field measurements in a shunting yard environment, and a comprehensive evaluation of the collected data. The results provide empirical evidence on the reliability and localization accuracy of a wide band T2T communication system in a complex railway scenario, demonstrating its potential as a core technology for VCTS and SDFW.

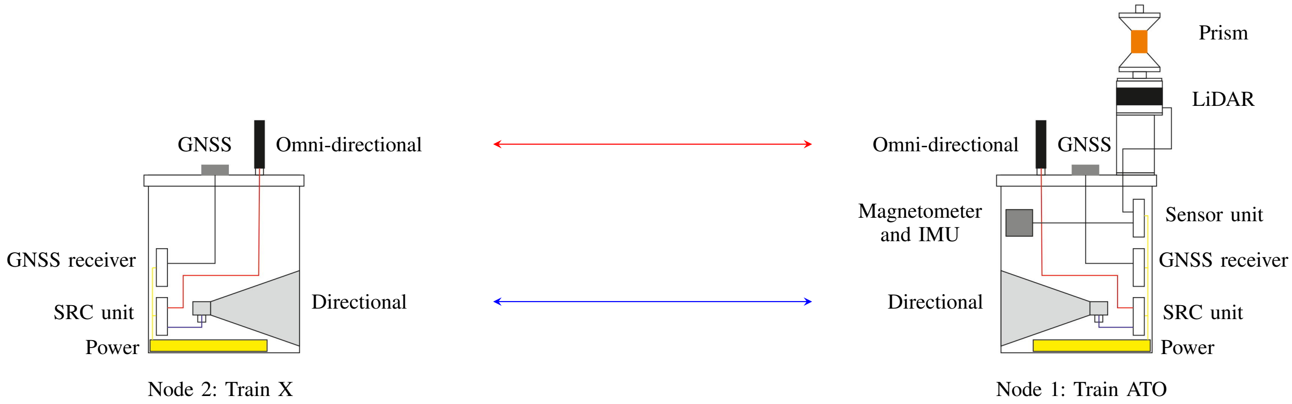

Fig. 1: SRC and RL system architecture with two nodes: Train X and Train ATO.

Fig. 2: Train X and Train ATO nodes mounted on the trains with Leica TS MS60 laser tracking infront.

II. Architecture

The SRC and RL system was designed to jointly enable data exchange and radio-based ranging between two communication nodes. The heart of each node is the SRC unit and the implemented RL algorithm. The architecture with the single elements is depicted in Figure 1

A. Short-range communication units

Each SRC unit is based on two Qorvo DW1000 ultra-wide band (UWB) transceiver chips. The integration of two chips and the resulting layout is a DLR development. This double chip integration enables two independent but synchronized communication threads with the possibility of connecting external antennas. For the railway tests, one omni-directional antenna and one directional antenna was used at each node. As omni-directional antenna, a Taoglas TU.60.3H31 [6] and for the directional antenna a Taoglas PHA.01.A [7] was used. To avoid interference, the omni-directional link was set to channel 2 (indicated in red in Figure 1), the directional link to channel 5 (indicated in blue in Figure 1).

B. Relative localization algorithms

As relative localization algorithm a double-sided two-way ranging scheme was implemented as presented in [8] . As stated in [8] this scheme allows a compensation for linear clock drifts of the communication nodes and increases the distance accuracy. For one distance estimation, both nodes are actively exchanging four time stamped communication packets started by the node with the lowest identifier (poll message), followed by an answer message of the second node. With the data exchange indicated as final, node 2 is able to calculate the distance to node 1. To allow node 1 derive a distance estimation as well, the recorded time stamps are transmitted from node 2 to node 1 in the additional data exchange called report [9]. Based on this exchange of time stamps, four time durations (run time ΔR and processing time ΔP at node 1 and 2, respectively) can be calculated, and thus, the distance

$$d = c\frac{(\Delta R_1 \cdot \Delta R_2)\,(\Delta P_1 \cdot \Delta P_2)}{\Delta R_1 + \Delta P_1 + \Delta R_2 + \Delta P_2} \tag{1}$$

between node 1 and node 2 can be estimated; c denotes the speed of light.

C. Reference system

The reference system fulfilled several tasks:

- Synchronization: All units within one node were synchronized to the global navigation satellite system (GNSS) time provided by a Network Time Protocol (NTP) server hosted by Septentrio PolaRx 5 GNSS receiver. The GNSS position was recorded as well, but not used for the presented evaluation. Due to limited space uBlox ANN-MB-00-00 antennas were mounted on top of each node.
- Reference position: To ensure a ground truth position in order of centimeters, the laser tracking system Leica Total Station MS60 was used. The MS60 tracked the prism mounted on the moving node 1 during all maneuvers and recored the position synchronized with GNSS time. The position of the static node 2 as well as static objects along the track were measured before the tests.
- Environment: The environment was scanned by a Velodyne VLP16 light detection and ranging (LiDAR) device. The LiDAR was only mounted on Node 1, as this node was moving at all test cases. In addition to the LiDAR, inertial measurement units (IMUs) including a magnetometer were installed to investigate future absolute and cooperative localization technologies for GNSS-denied areas. A first analysis is presented in [10].

TABLE I: Test cases, maneuvers and environments.

Test case				Train ATO			Train X		
#	Name	Maneuver	Environment	Position	Speed	Track	Position	Speed	Track
1	Coupling	Approaching on same track	Clear A	300-0	5-10	B	0	0	A or B
			Clear B	300-0	5-10	A	0	0	A or B
2	De-coupling	Departing on same track	Clear A	0-300	5-10	B	0	0	A or B
			Clear B	0-300	5-10	A	0	0	A or B
3	Fixed distance	Static on multiple positions	Clear A	10-260	0	B	0	0	B
4	Passing	On parallel tracks	Clear A	300-0	5-10	B	60	0	A
			Clear A	0-300	5-10	B	60	0	A
5	Coupled mode	Platoon driving	Clear A	350-70	5-10	B	280-0	5-10	B
			Clear A	70-350	5-10	B	0-280	5-10	B

III. Railway tests

The tests were planed and executed by DLR and the Nederlandse Spoorwegen (NS) within the FP2R2DATO project. DLR provided the test equipment, the reference system and the research staff, while NS provided the trains, the test drivers, the safety staff and the tracks. The tests were conducted in Amersfoort, Netherlands, within 3 days end of April 2025. The tests reported were carried out by qualified NS test drivers in a controlled environment.

A. Environment

As shown in Figure 2 the test environment was limited to two tracks with parked trains on the third track and a fence next to the first track. The first track next to the fence is referred to as Track A and the second track next to the parked trains as Track B. On this yard, all tracks are electrified and a buffer stop terminates each track in front of a railway maintenance building. The first 260 m of the tracks are straight followed by a turn to the right up to 400 m total length. Due to the turn, the fence was shadowing the line of sight signal for maneuvers considering large communication distances.

B. Test cases and maneuvers

The defined test cases reflect the train operation for VCTSs and small train units like SDFWs. For all test cases, the maneuvers and the environments are summarized in Table I and described in detail as follows:

- Test case 1+2: The coupling and de-coupling test cases reflect the approaching and departing phase of trains in a VCTS in a railway station, as well as the automated coupling and de-coupling of autonomous SDFWs in a shunting yard. One train was static, the second train was approaching or departing on the same track.
- Test case 3: The fixed distance test case was used as a reference case to investigate the effects on the SRC and the RL of moving nodes in comparison to purely static nodes. Every ten meters measurements were performed in a static setup for one minute.
- Test case 4: Virtual coupling enables the distribution of train units on parallel platforms in a station. Multiple SDFWs distributed on parallel tracks may coordinate themselves to leave the shunting yard as one freight train. For both applications, communication between nodes passing each other or distributed over several tracks is required. The passing maneuver reflects this complex situation and investigates the effects of shadowing by train bodies of trains on parallel tracks.
- Test case 5: This test case showcases two trains driving in a very short distance on the same track as if they would be part of a VCTS.

C. Implementation and schedule

The SRC unit, the antennas and the peripherals were installed in stand-alone boxes for each node as depicted in Figure 1. As indicated with the yellow boxes at the bottom of each box, power banks were installed to power the active units with 5V or 12V. In addition, LTE modems were installed to enable remote access and control to each node. In this way, the nodes were easy to handle and could be mounted on the couplers of the trains without additional cabling as shown in Figure 2. The remote access was also used to showcase the RL. The real time information of the estimated distance was presented to the train drivers on a screen in the driver's cab. This information was well received and assisted the train drivers for maneuver control.

NS provided the ATO test train SNG 3002 (Train ATO) for 3 days and an additional SNG train (Train X) for one day. With this availability of trains, preliminary static tests could be performed with Train ATO on the first day. On the second day, with both trains available, test cases 4 and 5 could be performed. On the third day, only Train ATO was available and Node 2 was mounted on a tripod in front of a buffer stop emulating Train X. With this setup test case 1, 2 and 3 could be performed with the largest possible communication range as mentioned in Table I. In total around 100 runs were performed covering roughly 30 km of testing.

On the second and third day, FP2R2DATO project representatives participated in the tests and a video team recorded the tests for documentation and public relations. A video can be watched at Youtube@DLR_KN [11].

IV. Evaluation

Figure 3 shows an example of 22 runs of test cases 1 and 2. The runs go forth and back from 250 m to roughly 3 m and back to 250 m. The occurrence of consecutive packet errors is plotted in the middle chart. The distance error is shown in the bottom chart. All three charts are plotted in relation to the test time.

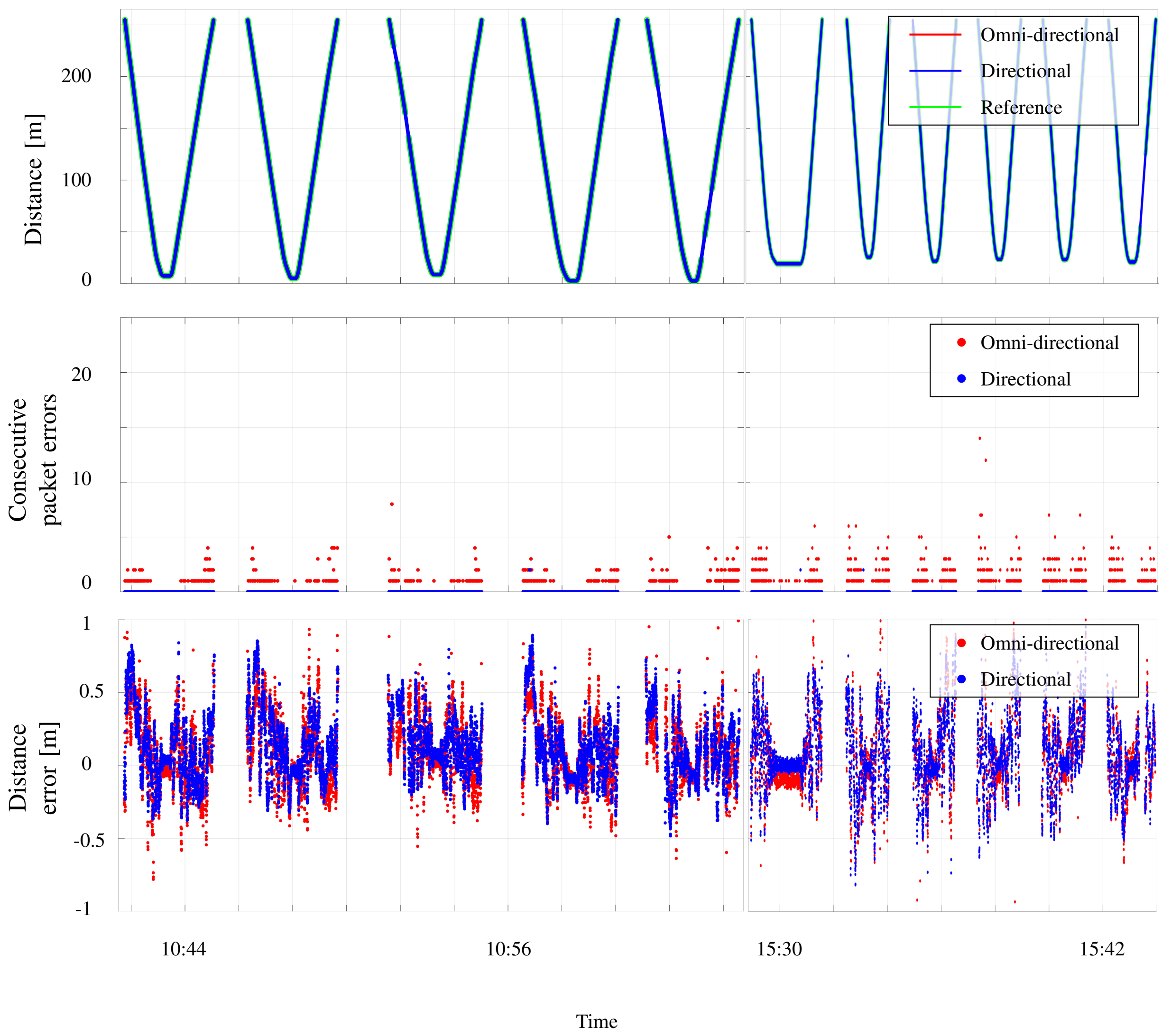

Fig. 3: Distance, consecutive packet errors and distance error over time for omni-directional and directional links.

A. Short-range communication

For maintaining a safe distance between two trains traveling closely together, not only the statistical error rate but also the age of information must be kept minimal. This goal can be achieved by using a high update rate at the transmitter and minimizing the occurrence of consecutive packet errors at the receiver. Since each communication device has a limited update rate, understanding and analyzing the occurrence of consecutive packet errors becomes crucial for ensuring reliable performance.

Out of Figure 3 it can be clearly seen that the sub-system based on omni-directional antennas experiences larger numbers of consecutive errors when the distance is increased. The sub-system based on directional antennas is hardly experiencing consecutive packet errors. Both the behavior of the omni-directional link indicated in red and the directional link indicated in blue can been seen in Figure 4. For the omni-directional antennas (shown in red), sparse instances of 2 to 5 consecutive packet errors are observed within the 0 to 80 m range. Beyond this, up to 200 m, the maximum number of consecutive missing packets reaches 12. At distances up to 250 m, the number of consecutive errors increases further, with a peak of up to 20 missing packets. In contrast, for the directional antennas (indicated in blue), the number of consecutive packet errors remains below two across the entire range from 3 to 250 m. A count of zero consecutive packet errors signifies a completely error-free transmission.

Figure 5 presents the packet error rate (PER) as a function of distance for both subsystems. The data points represent the accumulated PER from the 56 experimental runs, grouped into 10 m distance intervals. For the omni-directional antennas, the PER rises from approximately 10^{-3} at 10 m to around 10^{-1} by 80 m. From 80 m to 250 m, the PER fluctuates between 10^{-1} and $2 \cdot 10^{-1}$. The elevated error rates beyond 80 m are attributed to the railway environment, where metallic structures such as parked trains, overhead line masts, and

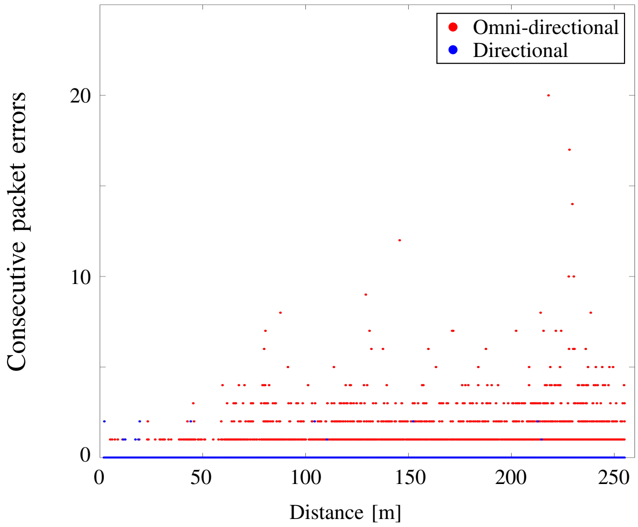

Fig. 4: Consecutive packet errors over distance.

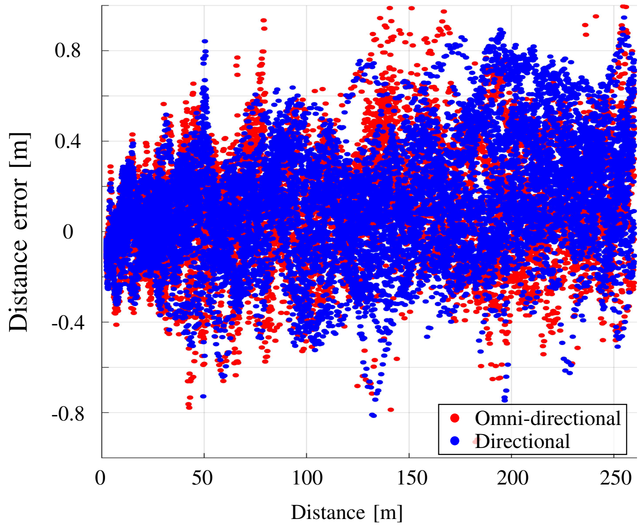

Fig. 6: Distance error over distance.

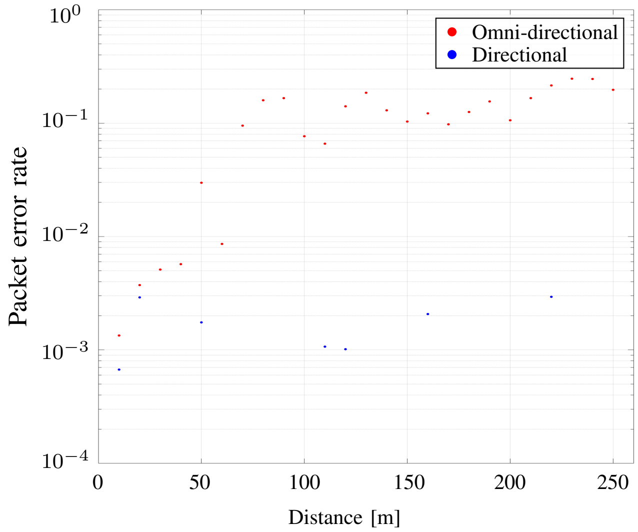

Fig. 5: Packet error rate over distance.

fencing generate multipath components (MPCs). The omni-directional receiver captures all these MPCs, leading to inter-symbol interference and, consequently, corrupted or unusable packet data. In contrast, the directional antennas exhibit a much lower PER, starting at $7 \cdot 10^{-4}$ and remaining between 10^{-3} and $3 \cdot 10^{-3}$ from 20 m to 250 m. Notably, several distance intervals such as 30, 40, 60, and 70 m lack blue dots, indicating that the PER was zero in those cases. The relatively higher PER observed at 10 m for directional antennas is due to receiver saturation caused by the high antenna gain. However, compared to omni-directional antennas, directional antennas receive only a small portion of the MPCs, primarily those aligned with the main beam. This selective reception significantly reduces interference and results in a substantial improvement in PER performance.

B. Relative localization

To evaluate the performance of the UWB-based double-sided two-way ranging distance estimation across varying train separations as shown in the bottom chart of Figure 3, the distance error is plotted against the actual distance in Figure 6. The results show a gradual increase in error, rising from approximately ±20 cm at 3 m to ±60 cm at 50 m, and further to ±80 cm at 250 m. Outliers are rare and remain within ±1 m, indicating high consistency. Both sub-systems, the one with the omni-directional and the one with directional antenna, show no major differences in the distance error. For both sub-systems a distance estimation could be provided within the whole SRC range of 250 m in this challenging railway environment.

The RL test evaluation showed an accuracy between ±20 cm to ±80 cm depending on the distance between the trains. The significant variation of up to ±1 m is primarily due to the impact of multipath effects in the railway environment on UWB signal transmission, combined with limitations in the accuracy of the ground truth reference system. Unfortunately, the ground truth positions were affected by multiple system outages, a reduced update rate while tracking, and substantial accuracy deviations of the Leica TS MS60. As a result, the expected accuracy of the reference system of better than 2 cm was not achieved in practice by far. For some test times, the ground truth accuracy was in the same order of magnitude as the achieved RL accuracy.

V. Conclusion

This work demonstrates the feasibility of T2T SRC and RL based on IEEE 802.15.4 for safety-critical rail applications such as VCTS and SDFW. Testing in a complex, real-world environment validates robust T2T communication and decimeter-level radio-based distance estimation (±20 cm to ±80 cm) over distances up to 250 m, even under challenging conditions including multipath and shadowing. A implementation of a more sophisticated channel estimation would reduce the multipath effects and enhance the distance estimation. Directional antennas significantly improve link reliability by reducing interference, while omni-directional configurations still ensured stable performance within operational ranges. The results confirm that wide band-based T2T SRC and RL enable high-availability of data exchange and accurate radio-based distance estimation, essential for gap supervision, dynamic spacing, and collision avoidance. The decentralized, infrastructure-independent nature of the system supports scalable, resilient, and autonomous train operations. These findings provide a strong technical foundation for future work on closed-loop control, failure analysis, certification, and integration into a unified decentralized communication framework for next-generation rail systems.

ACKNOWLEDGEMENT

We are very thankful for the outstanding collaboration with our project partner Nederlandse Spoorwegen (NS) within the project FP2R2DATO. Special thanks go to Ton Visser and Jeroen Braakman, both affiliated with NS, for providing the possibility of testing with moving trains, all the discussions, and the organization on NS side.

Funded by the European Union. Views and opinion expressed are however those of the authors only and do not necessarily reflect those of the European Union or the Europe's Rail Joint Undertaking. Neither the European Union nor the granting authority can be held responsible for them. The project FP2R2DATO is supported by the Europe's Rail Joint Undertaking and its members.

Co-funded by the European Union

REFERENCES

[1] J. Moreno García-Loygorri, J. Goikoetxea, E. Echeverria, A. Arriola, I. Val, S. Sand, P. Unterhuber, and F. del Rio, "The wireless train communication network: Roll2rail vision," *IEEE Vehicular Technology Magazine*, vol. 13, no. 3, pp. 135–143, 09 2018.

[2] A. Lehner, T. Strang, and P. Unterhuber, "Direct train-to-train communications at low uhf frequencies," *IET Microwaves, Antennas Propagation*, vol. 12, no. 4, pp. 486–491, 03 2018.

[3] P. Unterhuber, A. Lehner, and F. de Ponte Müller, "Measurement and Analysis of ITS-G5 in Railway Environments," in *Communication Technologies for Vehicles*, San Sebastian, June 2016, pp. 62–73. [Online]. Available: http://link.springer.com/10.1007/978-3-319-38921-9_7

[4] R. He, B. Ai, G. Wang, K. Guan, Z. Zhong, A. Molisch, C. Briso-Rodriguez, and C. Oestges, "High-Speed Railway Communications: From GSM-R to LTE-R," *IEEE Vehicular Technology Magazine*, vol. 11, no. 3, pp. 49–58, 09 2016.

[5] P. Unterhuber, "Test of IEEE802.15.4 for Train-to-Train Short Range Communication and Relative Localization," in *7th SmartRaCon Scientific Seminar*, vol. 7, October 2025, pp. 1–5.

[6] G. West, "Taoglas Omni-Antenna TU.60.3H31." [Online]. Available: https://www.taoglas.com/datasheets/TU.60.3H31.pdf

[7] Y. Y. Kai and C. Jack, "Taoglas Horn-Antenna PHA.01.A." [Online]. Available: https://www.taoglas.com/datasheets/PHA.01.A.pdf

[8] D. Neirynck, E. Luk, and M. McLaughlin, "An alternative double-sided two-way ranging method," in *2016 13th Workshop on Positioning, Navigation and Communications (WPNC)*, 2016, pp. 1–4.

[9] C. Gentner and M. Schmidhammer, "Ranging and multipath-enhanced device-free localisation with densely-meshed ultra-wideband devices," *IET Microwaves, Antennas & Propagation*, vol. 17, no. 8, pp. 667–676, 2023. [Online]. Available: https://ietresearch.onlinelibrary.wiley.com/doi/10.1049/mia2.12373

[10] B. Merk, B. Siebler, P. Unterhuber, A. Lehner, and S. Sand, "Cooperative Localization of Trains with Magnetic Field Measurements and Radio-based Ranging," in *VTC Spring 2026 - IEEE Vehicular Technology Conference*, 2026.

[11] German Aerospace Center (DLR), "FP2-R2DATO - Rail to Digital automated up to Autonomous Train Operation - Test Campaign Amersfoort," 2026. [Online]. Available: https://youtu.be/T424LpuiC9U?si=6P6bh3W7_GnGdWT4